

TEMPERATURE-STRESS COUPLING MECHANISM ANALYSIS OF ONE-TIME POURING MASS CONCRETE

by

Ben-Gao YANG^{a,b,c}, Peng HE^{a,b*}, Gao-You PENG^{a,b,c}, and Tong LU^{a,b,c}

^a College of Water Resource and Hydropower, Sichuan University, Chengdu, China

^b State Key Laboratory of Hydraulics and Mountain River Engineering,
Sichuan University, Chengdu, Sichuan, China

^c Key Laboratory of Deep Underground Science and Engineering, Sichuan University,
Ministry of Education, Chengdu, China

Original scientific paper

<https://doi.org/10.2298/TSCI180825231Y>

Thermal damage control of mass concrete is the key to guarantee the quality of mass projects. Based on several engineering experiences and finite element software ANSYS, the temperature field and stress field of the typical dam section of the Tengzigou hydropower station in Sichuan province were simulated. Considering the actual materials used, cooling measures, etc., maximum tensile stress and compressive stress at different time points derived from the temperature stress field during the time of concrete maintenance were calculated, and the numerical results showed that strength increment under the given conditions was much less than the actual condition. After the concrete of the dam body of the hydro power station were poured, there was no significant temperature stress crack appeared through a long-term observation, and the project condition was in tune with the calculated expectation. The above research results are valuable to further prediction of concrete temperature in different periods, the pre-study of the effect of temperature control measures, and these could offer guidance of the adjustment of temperature control measures in the case of abnormal conditions.

Key words: mass concrete, ANSYS, numerical simulation, temperature stress

Introduction

The mass concrete was widely used in the civil engineering industry and consumed in the annual hydraulic engineering reaches more than 10 million m³. It played an irreplaceable role in modern civil engineering [1]. However, in the early pouring and curing process, the temperature inside the concrete was easily generated due to its great thickness. The security of the structure was threatened. The control of temperature cracks in mass concrete had become a hot issue for scholars.

Wilson [2] took the lead in applying the 2-D finite element simulation program to analyze the temperature stress of mass concrete structures and successfully applied it to the temperature field calculation of Dworkshak Dam. The Wilson's program was improved and the temperature field simulation calculations on the Willow Creek Dam were performed [3]. the 3-D temperature stress analysis software ANACAPA was developed [4]. The possibility and severity of cracks in the project could be predicted by this software. The 3-D stress field of the Miyagase Dam was simulated [5] by using the finite element method and the difference method

* Corresponding author, e-mail: yangbgao@126.com

firstly. The thermochemical-damage-creep coupling model was used [6] to analyze the early mechanical properties of mass concrete. They claimed that the ambient temperature has an important influence on temperature stress. The models of massive block concrete and massive reinforced concrete wall models were analyzed [7]. Temperature gradients and basic constraints were found to be the main cause of temperature stress. A finite element simulation program based on hydration heat was developed [8, 9] to simulate the temperature distribution of early concrete in a large solid circular raft foundation. They discovered that the use of split pouring can significantly reduce the temperature level. A numerical model based on early cracking of concrete was developed [10]. It indicated that the mass concrete structure had high creep sensitivity. The concrete crack can be effectively controlled by limiting the maximum internal and external temperature difference of concrete, which is found [11]. As air cooling systems was introduced into large-volume concrete structures [12], the degree of cracking of the structure were reduced significantly.

The domestic temperature-stress coupling analysis of mass concrete started late. The temperature problem of concrete was first proposed [13]. Then, with the peak of the Chinese large-scale concrete structure construction, the analysis of mass concrete structure has entered a peak period. The effects of pouring temperature, ambient temperature and hydration heat on the internal temperature stress of concrete were analyzed in [14, 15]. They found that hydration heat was the main cause of temperature stress. Thermal-flow coupling analysis on mass concrete based on ABAQUS was carried out by using fine algorithm [16]. The research found that the results obtained by the fine algorithm were relatively large, which was beneficial to temperature control and crack prevention of the structure. The internal stress and displacement of mass concrete structures was simulated by using ABAQUS [17]. A multi-field coupled mathematical model was established to analyze the temperature field and stress field of the concrete dam by compiling a finite element program [18]. They found that the maximum temperature principal stress of the coupled block was larger. The influence of cooling water pipes was considered in [19]. The temperature field of mass concrete structures was simulated by him by using MIDAS, which provided guidance for the laying of cooling water pipes on site.

Due to the fact that various engineering conditions were not reproducible, therefore, numerical simulations of the project were still needed for specific projects. Taking the Tengzigou hydro power station as an example, the aim of the paper is to use the ANSYS to analyze the temperature-stress field coupling of the typical dam section of the Tengzigou hydro power station.

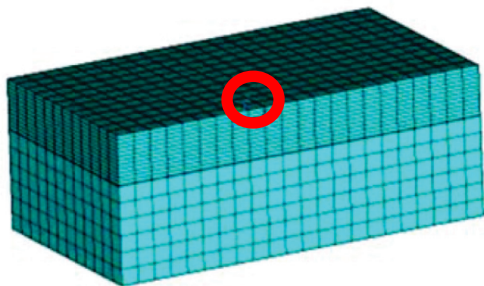


Figure 1. Computational entity and finite element model

Numerical Simulation

Establishment of numerical model

The model of this paper was based on the 27 warehouse of the 11[#] dam section of the typical dam section of the Tengzigou hydro power station. The length, width and height of the casting blocks were 22 m, 12 m, and 3 m, respectively, and the diameter of the cooling pipes were 32 mm, in order to satisfy the boundary condition of finite element calculation, the basis (poured) concrete took a length, width and height of 22 m, 12 m, and 6 m, as shown in fig. 1.

In the simulation calculation, the empirical formulas were all from Zhu Bofang's *temperature stress and temperature control of mass concrete* [1], which had achieved good prediction and calculation results in many engineering practices. The pouring temperature was 15 °C (design required temperature < 18 °C), the environment temperature was 25 °C, the cooling water temperature was 10 °C. The selection of relevant empirical values was shown in tab. 1. The indirect method was used for temperature stress coupling analysis. Therefore, different units were used in temperature field calculation and temperature stress. The SOLID70 in ANSYS was used in thermal analysis. Its degree of freedom was only temperature, which greatly increases the calculation speed. The temperature stress analysis selected SOLID45, which was 8 node structure unit, each node has 3° of freedom. This unit fully satisfied the calculation task. Using ANSYS automatic unit conversion realize two types of unit transition, in order to ensure a more accurate calculation result, all the mesh adopted 8-node hexahedron unit. A total of 5016 units and 5980 nodes were divided, of which 3168 were pouring units and 3887 were nodes. The pouring units became obviously denser. In this way, the total number of units could be reduced, the calculation speed could be improved, and an ideal calculation result could be obtained.

Table 1. Parameter selection

	Density [Kg ^m ⁻³]	Specific heat [JKg ⁻¹ °C ⁻¹]	Thermal conductivity [Jm ⁻¹ h ⁻¹ °C ⁻¹]	Linear expansion coefficient [m°C ⁻¹]	Elastic Modulus [Pa]	Poisson's ratio
Pouring block	2405	934	8108	9.52e-6	—	0.176
basis	2405	934	8108	9.52e-6	2.68e10	0.176

In the calculation process, in order to obtain the corresponding calculation results of each part of the block, 9 representative calculation monitoring points were arranged in the model, as shown in fig. 2.

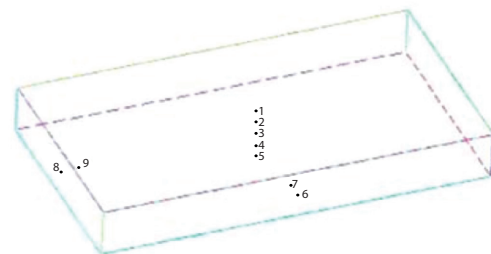


Figure 2. Calculation monitoring node lay-out

The boundary conditions of the temperature field were calculated as shown in fig. 3. The insulation effect of the surrounding steel formwork (according to Bofang) was negligible, so the surrounding and top boundary conditions were convection with air, and the cooling water was added to the bottom of the boundary to consider the influence of cooling measures such as laying water pipes on the pouring block.

The temperature-stress calculation boundary conditions were shown in fig. 4. The top surface was a free surface, there were templates around, the vertical displacement constraint was added besides the bottom surface was in contact with the foundation, and the they were deformed and co-ordinated.

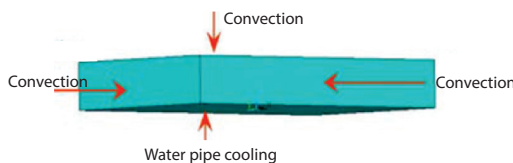


Figure 3. Temperature calculation boundary conditions

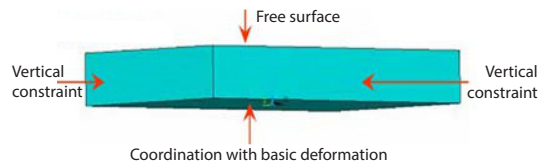


Figure 4. Temperature stress calculation boundary conditions

Analysis of temperature field of mass concrete

The temperature field analysis by ANSYS showed that the center of the pouring block reached the highest temperature on the 4th day after pouring. The maximum temperature in the center was 35.8 °C (which was less than the design temperature of 36 °C), the surface temperature was 28.1 °C, then the temperature began to decline. Due to the effect of the cooling water pipe, the highest temperature point did not appear in the center of the concrete, and it moved upwards by 0.5 m. The temperature gradient of the surface was less than the bottom of the cooling water pipe where the maximum temperature gradient occurred. We could find that the concrete temperature was almost close to the environment temperature on the 28th day after pouring concrete, and the temperature gradient was mostly generated by the cooling water, the maximum temperature gradient also appeared near the cooling water pipe.

As shown in figures 5-7, during the whole process of pouring cooling, the concrete as a whole heated up faster, and the internal temperature reached the maximum temperature around the 4th day. After reaching the peak, the cooling rate was also relatively fast. Therefore, attention should be paid to the temperature gradient of the crack, which caused by the internal temperature change of the concrete during the cooling process. The curve of temperature changed with time was a parabola with lower left deviation, and the temperature reached the highest temperature around the 4th day, then began to decline and balance with the environment temperature. Figure 8 showed that the adiabatic temperature rise was different. The temperature rose linearly in the first 4 days, and the maximum temperature reached 47 °C. On the 4th day after pouring concrete, the curve quickly approached the level.

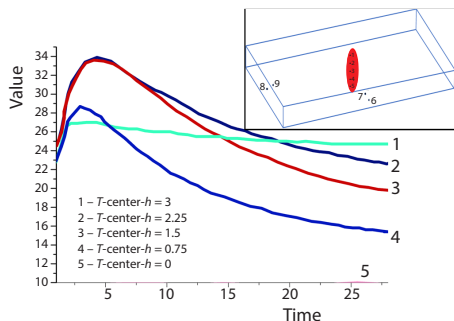


Figure 5. Comparison of the whole process of temperature changes of the first to 5th monitoring nodes

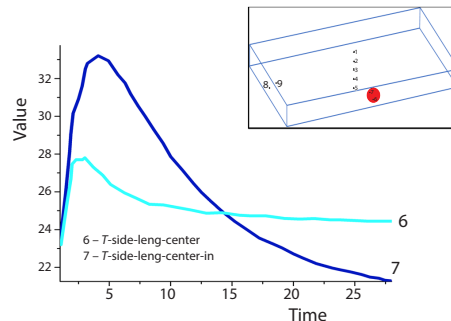


Figure 6. Comparison of the whole process of temperature changes of the of monitoring nodes 6 and 7

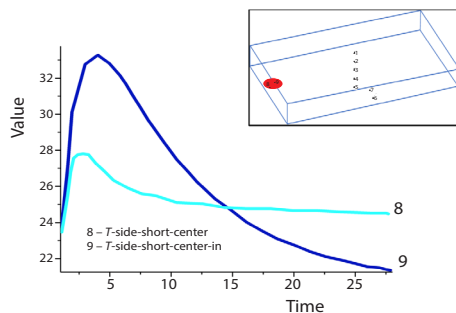


Figure 7. Comparison of the whole process of temperature changes of the 8th and 9th monitoring nodes

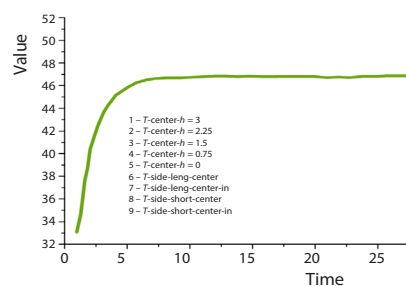


Figure 8. Adiabatic heating curve of each monitoring node

Analysis of temperature stress of mass concrete

On the 4th day after pouring concrete, the maximum tensile stress appeared on the upper part of the middle section around the periphery, and the value was less than 1 MPa, which did not satisfy the basic conditions of cracking. Compared with the area of maximum tensile stress, we found that the position of third principal stress was roughly the same, but the range was expanded and the maximum compressive stress reaches 5.28 MPa. Then a large-scale tensile stress area appeared on the upper surface of the pouring block at 28 days, because the surface was in contact with air. The thermal convection occurred, the temperature dropped rapidly, and the concrete internal temperature dropped slower, the temperature gradient between the inside and outside of the concrete was formed. But the tensile stress at this time was already very small. The range of the third principal stress was expanded on the 28th day after pouring concrete, the majority of the model appeared compressive stress, which was a result of the expansion deformation caused by the temperature rise.

Mass concrete temperature crack identification

The maximum tensile strength and maximum compressive strength of concrete in the same age were compared with the temperature stress value to determine whether the pouring block will crack. Figures 9 to 10 showed the relationship between the maximum tensile stress values of the monitoring nodes 1-9 at various ages and the tensile strength and compressive strength of concrete. The maximum tensile stress curves were between the compressive

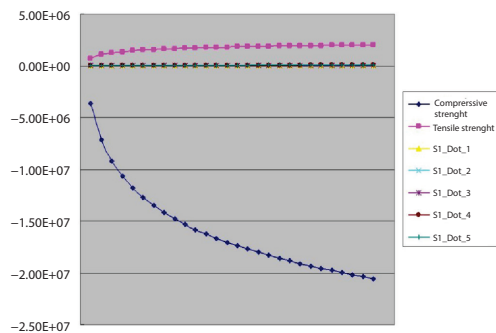


Figure 9. Relationship between compressive tensile strength and the S_1 of the first to 5th monitoring nodes

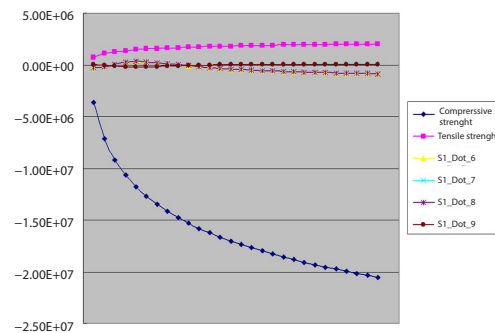


Figure 10. Relationship between compressive tensile strength and the S_1 of the 6th to 9th monitoring

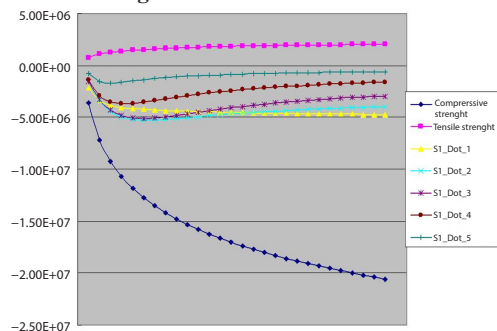


Figure 11. Relationship between compressive tensile strength and the S_3 of the first to 5th monitoring nodes

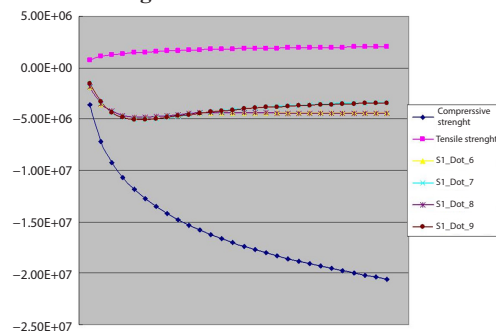


Figure 12. Relationship between compressive tensile strength and the S_3 of the 6th to 9th monitoring nodes

strength and the tensile strength. There was no intersection, and it was judged that the concrete will not crack. Figures 11 and 12 showed the relationship between the maximum compressive stress values of nodes 1-9 at various ages and the compressive strength and tensile strength of concrete. The maximum compressive stress change curve was much smaller than the tensile strength of concrete at the same time.

Through numerical simulation, it was found that the stress of each monitoring point was mainly compressive stress at each age. However, the compressive strength of concrete was often 10-18 times of its tensile strength, which was also much higher than the maximum compressive stress derived from the temperature change of concrete in the same age. As shown in figs. 11 and 12, it indicated the development of concrete compressive strength can fully resist the compressive stress caused by temperature difference.

Conclusion

Based on the calculation parameters and boundary conditions, set by the material test and construction conditions, the temperature stress field calculation of the typical concrete pouring block of the Tengzigou dam was completed. Making use of the actual materials, maximum tensile stress and compressive stress at different time points, the temperature stress field during the time of concrete maintenance were discussed in detail. On the 4th day after pouring, the maximum temperature of the concrete center reached 35.8 °C, which was less than the design temperature (36 °C). Due to the action of the cooling water pipe, the highest temperature was not in the center of the concrete, and the cooling water pipe was moved upwards by 0.5 m. At 28 days, the concrete temperature was almost closed to the environment temperature, and the temperature difference was mostly generated by the cooling water. Since the circumference and the top of the block were convective with the air, the temperature gradient became significantly larger at the periphery. Therefore, strengthening the surface insulation was an effective measure to prevent cracking. The temperature at each point reached the maximum temperature around the 4th day, and then began to fall. At last it balanced with the environment temperature. The adiabatic temperature rise was different. The temperature rose linearly in the first 4 days, and the maximum temperature reached 47 °C. After the 4th day, it gradually became gentle. The maximum temperature difference (10.8 °C) < allowable value (20 °C). The tensile and compressive stresses of each point were less than the compressive strength and tensile strength of the same age. The calculated maximum tensile stress was 0.3 MPa, which was less than the concrete tensile strength of 1.46 MPa in the same age. The maximum compressive stress was equal to 5.28 MPa, which was less than the concrete resistance of the same age. The compressive strength was 12.7 MPa. In the case of four-sided restraint, the overall performance was compressive stress. The overall stress state was beneficial to counteract the congenital deficiency of the concrete tensile strength and reduce the possibility of cracking.

Acknowledgment

This work was financially supported by the National Natural Science Foundation of China (51822403) and Sichuan International Technological innovation Cooperation Project (2018HH0159)

References

- [1] Zhu, B. F., *Temperature Stress and Temperature Control of Mass Concrete*, China Electric Power Press, Beijing, China, 1999
- [2] Wilson, E. L., *The Determination of Temperatures Within Mass Concrete Structures: A Report of an Investigation*, University of California, Structural Engineering Laboratory, California, USA, 1968

- [3] Tatro, B., et al., Thermal Considerations for Roller Compacted Concrete, *Journal of the American Concrete Institute*, 82 (1985), 3, pp. 32-38
- [4] Barrett, P. K., et al., Thermal Structure Analysis Methods for RCC Dams, *Proceedings*, Conference of Roller Compacted Concrete III, Sam Diedo, Cal., USA, 1992, pp. 389-406
- [5] Tohru, K., Investigations on Determining Thermal Stress in Massive Concrete Structure, *ACI Materials Journal*, 93 (1996), 1, pp. 96-101
- [6] Honorio, T., et al., Factors Affecting the Thermo-Chemo-Mechanical Behaviour of Massive Concrete Structures at Early-Age, *Materials and Structures*, 49 (2016), 8, pp. 3055-3073
- [7] Klemczak, B. A., Modelling Thermal-Shrinkage Stresses in Early Age Massive Concrete Structures-Comparative Study of Basic Models, *Archives of Civil and Mechanical Engineering*, 14 (2014), 4, pp. 721-733
- [8] Kuriakose, B., et al., Early-Age Temperature Distribution in a Massive Concrete Foundation, *Procedia Technology*, 25 (2016), Sept., pp. 107-114
- [9] Kuriakose, B., et al., Modelling of Heat of Hydration for Thick Concrete Constructions-A Note, *Journal of Structural Engineering*, 42 (2015), 4, pp. 348-357
- [10] Hilaire, A., et al., Modelling Basic Creep in Concrete at Early-Age under Compressive and Tensile Loading, *Nuclear Engineering and Design*, 269 (2014), 4, pp. 222-230
- [11] Lawrence, A. M., et al., Effect of Early Age Strength on Cracking in Mass Concrete Containing Different Supplementary Cementitious Materials: Experimental and Finite-Element Investigation, *Journal of Materials in Civil Engineering*, 24 (2012), 4, pp. 362-372
- [12] Azenha, M., et al., Application of Air Cooled Pipes for Reduction of Early Age Cracking Risk in a Massive RC Wall, *Engineering Structures*, 62-63 (2014), 3, pp. 148-163
- [13] Zhu, B. F., Temperature Calculation of Concrete Dam, *China Water Conservancy*, (1956), 11, pp. 8-20
- [14] Wang, J. X., et al., Finite Element Analysis on the Temperature Field of the Massive Concrete Anchorage of HaiCang Bridge, *China Railway Science*, 30 (2009), 5, pp. 46-52
- [15] Sun, Z. Z., et al., Finite Element Simulation of inside-outside Temperature Gradient and Thermal Stress for Abutment Mass Concrete, *Journal of Traffic and Transportation Engineering*, 16 (2016), 2, pp. 18-26
- [16] Liu, X. H., et al., The Refined Numerical Simulation of Pipe Cooling in Mass Concrete Based on Heat-Fluid Coupling Method, *Engineering Mechanics*, 29 (2012), 8, pp. 159-164
- [17] Huang, Z. Q., et al., Numerical Simulation of Hollow Pier Template of Highway Based on ABAQUS, *Journal of ShenYang University of Technology*, 38 (2016), 1, pp. 109-114
- [18] Yan, J., et al., Research on Thermal Stress of Mass Concrete under Hydro-Thermo-Mechanical Coupling During Initial Impoundment, *Journal of Hunan University (Natural Sciences)*, 43 (2016), 5, pp. 30-38
- [19] Zhuang, G. Q., Analysis of Heat of Hydration in Massive Concrete for Pile Caps, *Journal of JiuJiang University (Natural Sciences)*, 32 (2016), 3, pp. 35-39